Journal of Hazardous Materials 448 (2023) 130898

Contents lists available at ScienceDirect

Journal of Hazardous Materials

journal homepage: www.elsevier.com/locate/jhazmat

Metagenomic analysis characterizes resistomes of an acidic, multimetal (loid)-enriched coal source mine drainage treatment system

Qiang Huang [a], Ye Huang [b,c], Bao Li [a,c], Xiutong Li [b,c], Yuan Guo [a], Zhen Jiang [b,c], Xiaoling Liu [a], Zhenni Yang [b], Zengping Ning [a], Tangfu Xiao [d], Chengying Jiang [b,c,*], Likai Hao [a,c,e,**]

[a] State Key Laboratory of Environmental Geochemistry, Institute of Geochemistry, Chinese Academy of Sciences, Guiyang 550081, PR China
[b] State Key Laboratory of Microbial Resources, Institute of Microbiology, Chinese Academy of Sciences, Beijing 100101, PR China
[c] University of Chinese Academy of Sciences, Beijing 100049, PR China
[d] Ministry of Education, School of Environmental Science and Engineering, Guangzhou University, Guangzhou 510006, PR China
[e] CAS Center for Excellence in Quaternary Science and Global Change, Xi'an 710061, PR China

HIGHLIGHTS

- Resistome characteristics of a coal source AMD passive treatment were investigated.
- Multidrug efflux mechanism dominated antibiotic resistome.
- MGEs exerted more effluence on dynamic of MRGs than that of ARGs.
- Potential pathogens carrying multi-RGs were found.
- passive treatment decreased relative abundance of RGs to different degree.

GRAPHICAL ABSTRACT

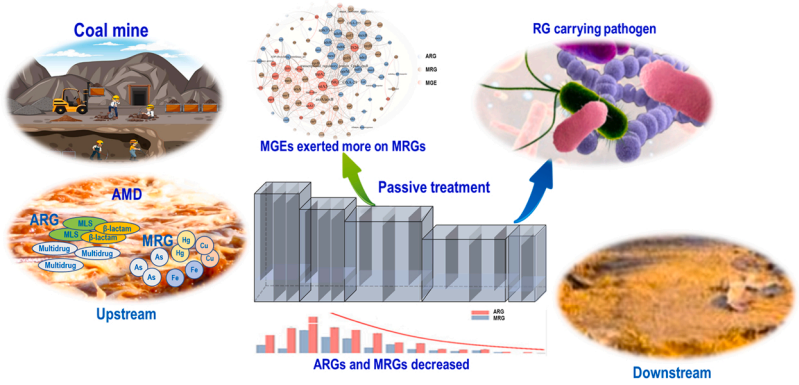

ARTICLE INFO

Editor: Jörg Rinklebe

Keywords:
Resistome
Co-selection
Coal source acid mine drainage

ABSTRACT

Heavy metal(loid) contaminations caused by mine activities are potential hot spots of antibiotic resistance genes (ARGs) because of heavy metal(loid)-induced co-selection of ARGs and heavy metal(loid) resistance genes (MRGs). This study used high-throughput metagenomic sequencing to analyze the resistome characteristics of a coal source acid mine drainage passive treatment system. The multidrug efflux mechanism dominated the antibiotic resistome, and a highly diverse heavy metal(loid) resistome was dominated by mercury-, iron-, and arsenic–associated resistance. Correlation analysis indicated that mobile gene elements had a greater influence

Abbreviations: AMD, acid mine drainage; ARG, antibiotic resistance gene; HGT, horizontal gene transfer; MAG, metagenome-assembled genome; MGE, mobile gene element; MRG, metal(loid) resistance gene; RG, resistance gene; ORF, open reading frame; MLS, resistance-nodulation - cell division; RND, resistance-nodulation-cell division.

* Corresponding author at: State Key Laboratory of Microbial Resources, Institute of Microbiology, Chinese Academy of Sciences, Beijing 100101, PR China.
** Corresponding author at: State Key Laboratory of Environmental Geochemistry, Institute of Geochemistry, Chinese Academy of Sciences, Guiyang 550081, PR China.
E-mail addresses: jiangcy@im.ac.cn (C. Jiang), haolikai@mail.gyig.ac.cn (L. Hao).

https://doi.org/10.1016/j.jhazmat.2023.130898
Received 22 November 2022; Received in revised form 7 January 2023; Accepted 27 January 2023
Available online 30 January 2023

Multiple metal(loid) contaminations
Passive treatment

on the dynamic of MRGs than ARGs. Among the metagenome-assembled genomes, six potential pathogens carrying multiple resistance genes resistant to several antibiotics and heavy metal(loid)s were recovered. *Pseudomonas* spp. contained the highest numbers of resistance genes, with resistance to two types of antibiotics and 12 types of heavy metal(loid)s. Thus, high contents of heavy metal(loid)s drove the co-selection of ARGs and MRGs. The occurrence of potential pathogens containing multiple resistance genes might increase the risk of ARG dissemination in the environment.

1. Introduction

Antibiotic resistance in microorganisms caused by antibiotic misuse and overuse threatens global public health [18,77]. The problem has gradually been recognized, and actions (such as limiting antibiotic use in stock farming and clinics) have been taken to control the spread of antibiotic resistance genes (ARGs) [37,58]. However, as antibiotic use control has not effectively reduced antibiotic resistance proliferation, it is now considered that other factors can also contribute to the environmental diffusion of ARGs [28]. In addition, increasing evidence have shown that nonantibiotic agents such as heavy metal(loid)s can also lead to ARGs emergence because of the co-selection of antibiotics and heavy metal(loid)s [40,6,61]. Based on co-selection theory, heavy metal(loid)s can affect not only the occurrence of corresponding heavy metal(loid) resistance genes (MRGs) but also other ARGs through mechanisms of co-resistance, cross-resistance, and co-regulation [36,45,68]. Ji et al. [29] even reported that some ARGs correlate more strongly with heavy metal(loid)s than with corresponding antibiotics. Therefore, metal (loid)-enriched environments may be potential reservoirs of resistance genes (RGs). The problem becomes more concerning because of the persistent co-selection pressure with heavy metal(loid)s that are harder to be transformed than antibiotics in natural environments [60,62].

Mining activities generate large amounts of mine tailings and acid mine drainage (AMD), which are ideal settings for studying metals' effects on ARGs. AMDs are the most typical metal(loid)-enriched environments and are characterized by extremely low pH (<4) and high concentrations of SO_4^{2-} and metal(loid) ions [32]. A global study recently reported that mining-impacted environments have multidrug resistance-dominated ARG resistome, with ARGs abundances nearly equal to those of urban sewage but much higher than those of freshwater sediments [72]. The study confirmed the hypothesis that metal (loid)-enriched environments are potential RG reservoirs, achieving huge improvements in helping understand the resistome characteristics of mine-environments. Yet, there is a minor drawback. As that study focused mainly on copper, Lead-Zinc, gold, pyrite and polymetallic, we are far from understating the resistome characteristics of coal source AMD. As one of the most important global energy sources, its substantial long-term demand has resulted in large-scale mining activities and severe AMD problems [38]. The coal source AMD may be another source of potential ARG reservoirs, but relative study has not been reported.

Different treatment systems have been developed to minimize AMD-caused environmental pollution. Passive treatments are the most promising tool because of relatively low input costs and easy maintenance [3]. In Guizhou Province in Southwestern China, a pilot-scale passive treatment system was constructed in 2013 for in-situ bioremediation of AMD. In a recent report, Chen et al., [15] analyzed variation in microbial communities along the system and evaluated its performance in removing Fe(II), while ignoring characteristics of resistome profiles in this treatment. Therefore, this study focused on this treatment system, investigated the resistome characteristics of the coal source AMD, analyzed correlations among ARGs, MRGs, mobile gene elements (MGEs), and environmental parameters, as RG's dissemination between bacterial cells were mediated by MGEs [70], and environmental parameters such as pH were reported to influent dynamics of RGs directly or indirectly [78], We collected samples from different ponds of the passive treatment and metagenomic techniques and geochemical measurements were conducted. Specifically, we aimed to: (1) investigate resistome characteristics of the coal source AMD; (2) analyze hosts of the main RGs; and (3) determine the role of MGEs in driving dynamics of ARGs and MRGs. Our study provides initial insight into the resistome characteristics of the passive treatment system and the potential risks of RG proliferation in coal source AMD-associated environments.

2. Materials and methods

2.1. Sample collection and processing

Samples were collected from an AMD passive treatment system of a coal mine (26°31′28.68″N, 106°34′13.72″E) in Guizhou Province in southwestern China. The AMD flows from the mine adit into five ponds of the treatment system in succession. Fig. 1 shows a schematic and photographs of the five ponds and six sampling sites. The six sampling sites were at the influent of the first pond and outlets of all five ponds, named as Entrance, Pond1, Pond2, Pond3, Pond4, and Effluence, respectively. At each site, three samples were collected below the water surface (0–30 cm). Main anions and cations were measured for every sampling point, and 16 S rRNA amplicon sequencing and metagenomic sequencing were performed.

pH and dissolved oxygen (DO) at each sample point were measured in situ with a multi-parameter Water Quality Analyzer (YSI, Ohio, USA). From each sample, 200 mL of water was filtered through a 0.45-μm sterile microporous filter membrane (Millipore, Massachusetts, USA) and separated into four 50-mL sterile centrifuge tubes to determine main anions and cations. To measure Mn, 50-mL samples were acidified with concentrated nitric acid (16 mol/L) and determined with an inductively coupled plasma-optical emission spectrometry (ICP-OES) analyzer (Optima 5300 DV, PerkinElmer, USA). To measure trace elements, 50-mL water examples were acidified with concentrated hydrochloric acid (12 mol/L) and then determined with inductively coupled plasma mass spectrometry (ICP-MS, PerkinElmer, USA). For SO_4^{2-}, samples were directly measured with ion chromatography (ICS-90, Dionex, USA). A ferrozine method was used to measure Fe^{2+} and total Fe [63]. Values of environmental parameters and concentrations of heavy metal(loid)s are presented as the mean ± standard error.

2.2. DNA isolation, amplicon sequencing, metagenomic sequencing, and bioinformatic analyses

Approximately 5 L of raw water from each sample was filtered through a 0.22-μm sterile microporous filter membrane (Millipore, USA). Membranes were stored separately in sterile centrifuge tubes in a foam box with dry ice and sent to Sangon Biotech Company (Shanghai, China) to extract DNA using an E.Z.N.A™ DNA kit (M5635–02, Omega, USA) based on its protocol.

In amplicon sequencing, the V3-V4 regions of the bacterial 16 S rRNA gene were amplified by polymerase chain reaction (PCR) using the paired primers 341 F/805 R with 2 × Hieff® Robust PCR Master Mix (Yeasen, China). Sequencing was conducted on an Illumina HiSeq 2500 platform. The returned merged sequences were used directly in subsequent analysis with the free online platform Qiime2 (v2021.4, qiime2.org) [11], mainly following the established protocol. Briefly, dada2 arithmetic was used to generate amplicon sequence variants (ASVs with clustering at 100% similarity) [13], and the latest Silva database (v138, not weighted) [9,54] was used to conduct taxonomic annotation.

Shotgun metagenomic sequencing of the 18 samples was conducted on an Illumina HiSeq 2500 platform with model of PE150, and the minimum sequencing depth was set at 10 Gb. The pipeline of Kneaddata (v0.6.1) (github.com/biobakery/kneaddata) embedded with Trimmomatic (v0.39) [10] was used to conduct quality control and host contamination filtration (key parameters were set as –trimmomatic-options 'ILLUMINACLIP: adapters/TruSeq3-PE.fa:2:40:15 SLIDINGWINDOW:4:20 MINLEN:50'). MEGAHIT (v1.1.3) was used to assemble reads into contigs, with kmer parameters set as –k-min 27, –k-max 141, and –k-step 12 and the minimum length of quality contigs set at 200 bp [35]. With the high-quality contigs, ORF (open reading frame) prediction, redundancy deletion, and counts quantification were performed by Prodigal (v2.6.3, with default parameters) [27], CD-HIT (v4.8.1, -aS 0.9 -c 0.95 -G 0 -g 0 -T 0 -M 0) [22], and Salmon (v0.13.1, with default parameters) [50], respectively.

Diamond (v2.0.2) with blastp model was used to detect ARGs and MRGs by blasting protein sequences in the SARG Database [73] and the BacMet2 Database [46], respectively, with parameters set as identity $\geq 70\%$, e-value $= 10^{-5}$, and alignment length ≥ 20. Blastn (v2.5.0 +) was used to detect MRGs by blasting nucleotide sequences (predicted ORFs) in the MobileGeneitcElement Database [49], with parameters set as identity $\geq 70\%$, e-value $= 10^{-5}$, and alignment length ≥ 28 and the blasting strand set as both. The CARD Database was used as a reference for the ARG mechanism category classification [30]. Abundance (coverage, ×/Gb) of RGs or MGEs in each sample was calculated based on the following formula [50]:

$$Relative\ abundance(coverage, \times/Gb) = \sum_{1}^{n} \frac{N_{mapped\ reads} \times L_{reads} / L_{RG/MGE-like\ ORF}}{S}$$

where $N_{mapped\ reads}$ is the number of the reads mapped to RG/MGE-like ORFs; L_{reads} is the sequence length of Illumina reads, which was 150 in this study; $L_{RG/MGE\text{-}like\ ORF}$ is the sequence length of target RG/MGE-like ORFs; n is the number of different RG/MGE-like ORFs belonging to the same RG/MGE types, which was calculated by Salmon in this study; and S is the size of the data set (Gb), which is the average of forward clean reads and reverse clean reads of each sample.

Contigs longer than 1000 bp were used to carry out metagenome assembly separately according to sampling sites with the MetaWRAP pipeline (v1.3.2) [67]. The pipeline includes several modules and can conduct MAG assembly, refinement, and quantitation separately. The software checkM (v1.0.12) [48] was used to determine the completeness and contamination of MAGs. High-quality MAGs (contamination < 5%, completeness > 70%) were used to detect RGs and MGEs, and taxonomic annotation was conducted by GTDB-Tk (v2.0.0) with its reference database (version release_207) [47].

2.3. Statistical analyses and visualization

R (v3.6.1) were used for statistical analysis and data visualization. Bar plots were drawn using a free online platform (ImageGP, ehbio.com). ANOSIM analysis (with Bray-Curtis distance), RDA analysis (with hellinger), Procrustes analysis and Spearman correlation heat map analysis were performed for comparing the difference of these samples on the free online platform (Tutools, cloudtutu.com). All qualified bacterial MAGs were collected to draw phylogenetic tree in the online platform iTOL (itol.embl.de), the tree file was produced by GTDB-Tk (v2.0.0) based on 120 bacterial marker genes. Network diagrams were drawn with the software Gephi (v0.9.2, github.com/gephi), and relative network properties were calculated by the same software. Matrix files were generated with the R package psych (v2.1.3), and the parameters were set as use = pairwise, method = Spearman, adjust = fdr, alpha = 0.05, $p < 0.05$, and $r > 0.7$. Abundances of RGs and MGEs are presented as the mean ± standard error.

2.4. Nucleotide sequence accession numbers

Sequences have been submitted to the National Center for Biotechnology Information BioProject with accession numbers PRJNA755874 and PRJNA785287, including 18 metagenome samples (raw paired sequences) and 18 16 S rRNA amplicon samples (clean merged sequences). Sequence data release date was October 1st, 2022.

3. Results

3.1. Characteristics of pH, SO_4^{2-}, dissolved oxygen, and heavy metal (loid)s at different sample sites

Table 1 shows the dataset of pH, DO, and concentrations of SO_4^{2-} and eight heavy metal(loid)s (iron includes total Fe and Fe^{2+}) at the six sampling sites. Detailed information on each sample is provided in

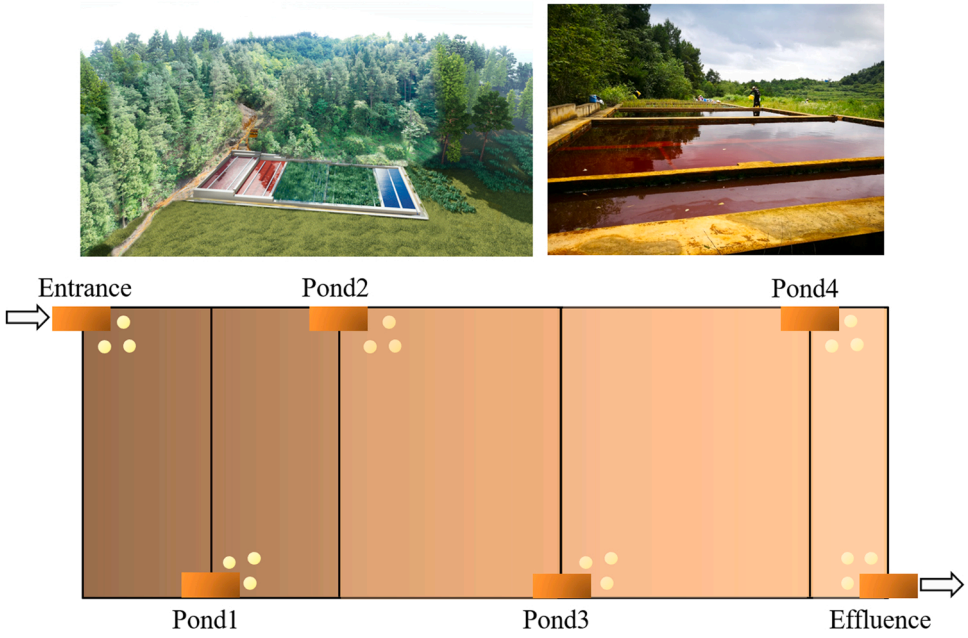

Fig. 1. Photographs of five ponds and schematic of the passive treatment of coal source acid mine drainage. Six sampling sites were at the entrance of the first pond and the effluences of five ponds, named as Entrance, Pond1, Pond2, Pond3, Pond4, and Effluence, respectively.

Table 1
Water pH, dissolved oxygen (DO), and concentrations of SO_4^{2-} and main metal(loid) elements at different sample sites in the passive treatment of coal source acid mine drainage. Values are the mean ± standard error.

Phases	Entrance	Pond1	Pond2	Pond3	Pond4	Effluence
pH	3.03 ± 0	3.00 ± 0.00	2.97 ± 0.00	3.04 ± 0.00	3.08 ± 0.00	3.13 ± 0.00
SO_4^{2-} (mg L^{-1})	4030.23 ± 199.93	5337.03 ± 418.19	6167.26 ± 355.75	6122.6 ± 32.22	6217.91 ± 16.76	6060.09 ± 209.79
DO (mg L^{-1})	4.19 ± 0.09	4.3 ± 0.07	5.05 ± 0.11	4.73 ± 0.05	3.05 ± 0.05	3.86 ± 0.01
Fe^{2+} (mg L^{-1})	0.71 ± 0.07	0.77 ± 0.07	0.85 ± 0.05	0.65 ± 0.02	0.73 ± 0.04	0.72 ± 0.02
Fe (mg L^{-1})	5.92 ± 0.08	22.14 ± 0.98	21.20 ± 3.93	16.48 ± 0.13	14.37 ± 0.09	14.55 ± 0.03
Mn (mg L^{-1})	13.22 ± 0.17	14.08 ± 0.22	12.27 ± 0.11	20.30 ± 2.22	20.51 ± 4.49	20.82 ± 4.42
Zn (μg L^{-1})	298.51 ± 6.46	291.27 ± 3.82	282.06 ± 10.97	301.88 ± 1.01	354.50 ± 13.45	347.03 ± 6.50
As (μg L^{-1})	1.60 ± 0.49	0.70 ± 0.22	1.70 ± 0.142	2.38 ± 0.25	3.14 ± 0.71	4.41 ± 0.12
Hg (μg L^{-1})	0.37 ± 0.24	0.06 ± 0.02	0.01 ± 0.01	0.05 ± 0.02	1.03 ± 0.74	2.04 ± 0.46
Cu (μg L^{-1})	8.16 ± 0.28	7.78 ± 0.11	9.63 ± 0.24	15.98 ± 0.19	26.58 ± 3.88	26.38 ± 0.46
Sb (μg L^{-1})	1.91 ± 2.09	0.13 ± 0.08	0.08 ± 0.03	0.36 ± 0.02	3.91 ± 1.62	5.20 ± 0.38
Pb (μg L^{-1})	1.84 ± 0.74	0.99 ± 0.10	1.59 ± 0.31	1.45 ± 0.23	14.94 ± 8.71	24.22 ± 1.70

Supplementary Table S1. The value of water pH increased slightly from 3.03 ± 0.00 at the influent to 3.13 ± 0.00 in the effluent. DO increased from 4.19 ± 0.09 mg L^{-1} at the influent to 5.05 ± 0.11 mg L^{-1} in sampling site of Pond 2 and then decreased to 3.86 ± 0.01 mg L^{-1} in the effluent. Concentration of SO_4^{2-} increased from 4030.23 ± 199.93 mg L^{-1} at the influent to 6060.09 ± 209.79 mg L^{-1} in the effluent. Concentration of Fe^{2+} changed slightly through the system, whereas total Fe increased from 5.92 ± 0.08 mg L^{-1} at the influent to 22.14 ± 0.98 mg L^{-1} in sampling site of Pond 1 and then decreased to 14.55 ± 0.03 mg L^{-1} in the effluent. Concentrations of the heavy metal(loid)s Mn, Zn, As, Hg, Cu, antimony (Sb), and Pb decreased but then elevated as AMD flowed from the influent to the effluent.

To summarize, pH, DO, and Fe^{2+} changed slightly throughout the system, whereas the other elements increased by different degrees from the influent to the effluent. As for microbial communities, Fig. S1 and Table S2 show the characteristics of microbial communities in different sampling sites.

3.2. Characteristics of resistomes and mobile gene elements at different sample sites

In ANOSIM analysis (Figs. S2a, 2b and 2c), significantly positive R values meant that dissimilarities between groups were bigger than dissimilarities within groups, revealed significant variations of RGs and MGEs when AMD flowed through these six sites.

Fig. 2a, 2b and Table S3 show ARG characteristics and variations. Sixty-nine types of ARGs resistant to 18 types of antibiotics were detected, including some clinically meaningful antibiotic groups, such as multidrug (30 ARGs), beta-lactams (8 ARGs), and the so-called last resort, vancomycin (4 ARGs). Multidrug-type ARGs predominated and

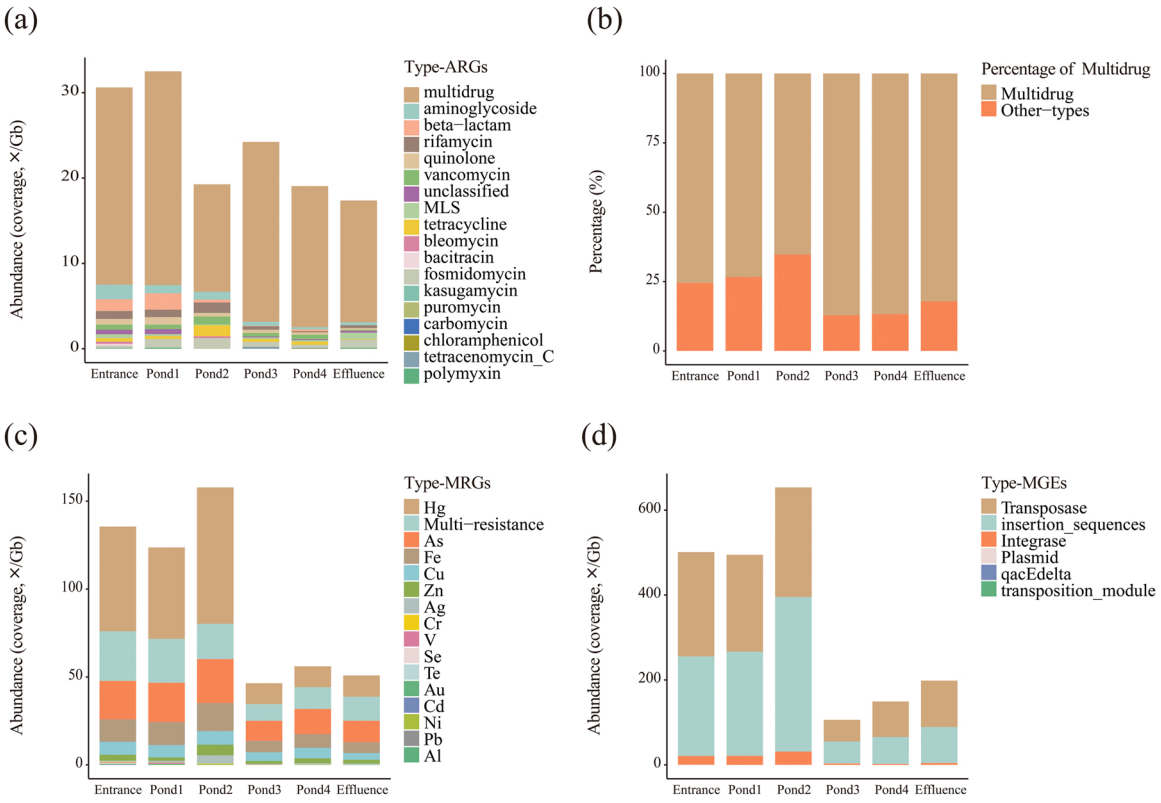

Fig. 2. Characteristics and dynamics of (a) antibiotic resistome (ARGs, antibiotic resistant genes) and (b) average percentage of multidrug-resistant ARGs and other types in six sample sites of the passive treatment of acid mine drainage. Characteristics and dynamics of (c) heavy metal(loid)s resistome (MRGs, heavy metal(loid) resistance genes), and (d) mobile gene elements (MGEs) in six sample sites. The six sample sites were at the entrance of the first pond and the effluences of five ponds, named as Entrance, Pond1, Pond2, Pond3, Pond4, and Effluence, respectively. The values are the mean abundance of each antibiotic type. In (a), MLS is macrolide–lincosamide–streptogramin. In (c), multi-resistance included resistance to 21 types of multimetal(loid)s.

accounted for over 65% of all sampling sites. Genes *mdtB*, *mexF*, and *mdtc* had the highest relative abundances, accounting for over 25% of total abundance. Total ARGs abundance decreased from 30.609 × /Gb at the influent to 17.368 × /Gb in the effluent, a decrease of 43.26%.

Fig. 2c and Table S4 show MRG characteristics and variations. Thirty-six types of MRGs (including 21 multimetal(loid) types) and 101 subtypes of MRGs (including 37 multimetal(loid) subtypes) were detected. The RG *fpvA* resistant to eight types of heavy metals was detected, including Cd, Co, Cu, Fe, gallium (Ga), Mn, Ni, and Zn based on BacMet2, but only in the sampling site of Entrance. The most abundant MRGs were those with Hg-, multiresistance-, As-, and Fe-related resistance, accounting for 21.23–49.15%, 12.74–26.86%, 15.82–25.46%, and 9.40–14.03%, respectively. For single MRG diversity, fourteen types of MRGs had Cu-related resistance, followed by those with As- (9), Hg- (8), and Fe (7)-related resistance. The MRG *merA* with Hg-related resistance had the highest relative abundance, followed

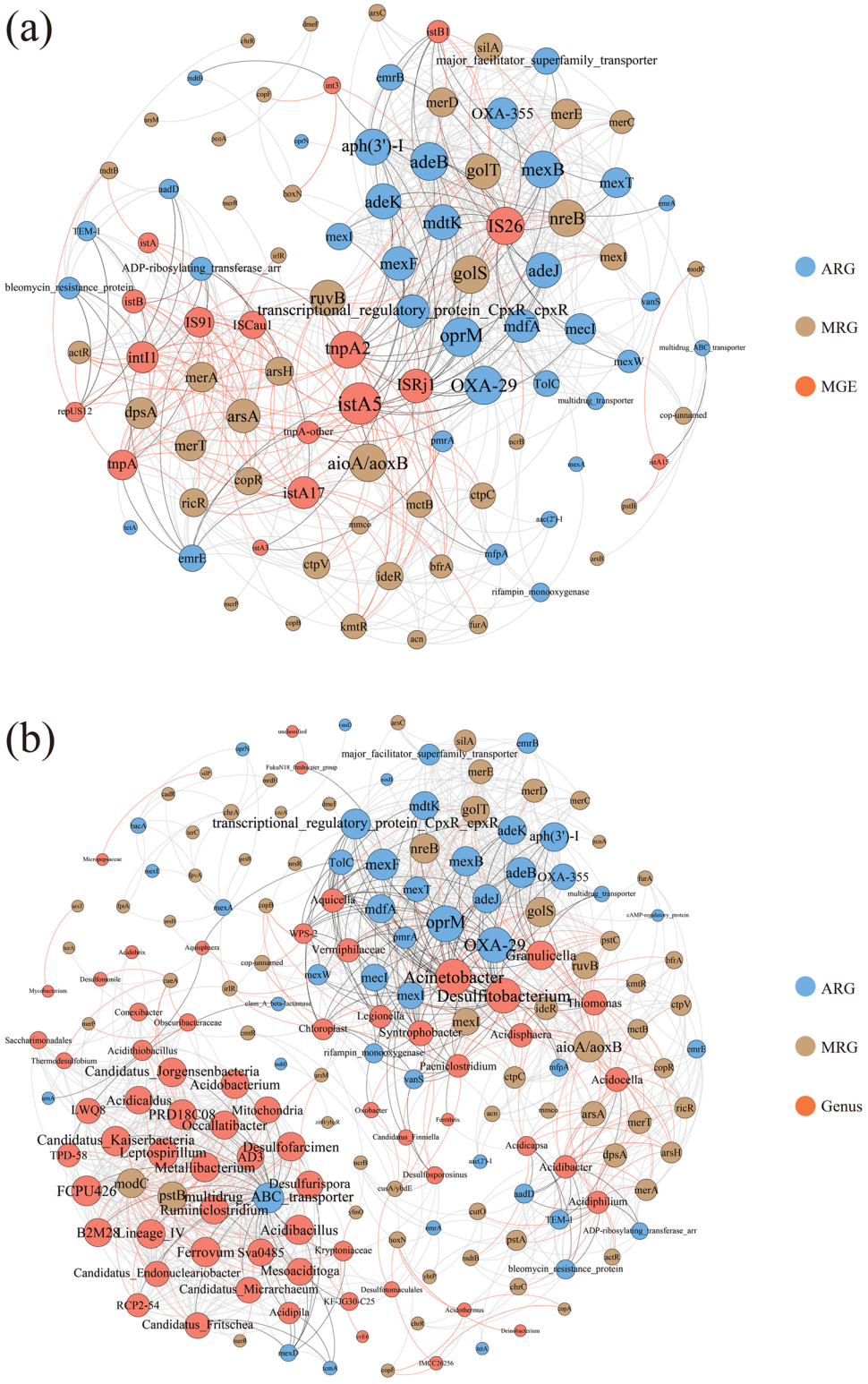

Fig. 3. (a) Co-occurrence relations among antibiotic resistance genes (ARGs), heavy metal (loid) resistance genes (MRGs), and mobile gene elements (MGEs) (Spearman correlations: $r > 0.7$, $p < 0.05$). (b) Co-occurrence relations among ARGs, MRGs, and genera (Spearman correlations: $r > 0.7$, $p < 0.05$). Blue nodes represent ARGs, brown nodes represent MRGs, and salmon nodes represent MGEs in (a) or genera in (b). The size of each node corresponds to the number of edges with other nodes. The red edges represent significantly positive correlations between MRGs and MGEs in (a) or between MRGs and genera in (b); the black edges represent significantly positive correlations between ARGs and MGEs in (a) or between ARGs and genera in (b); and the gray edges represent other significantly positive correlations between other types.

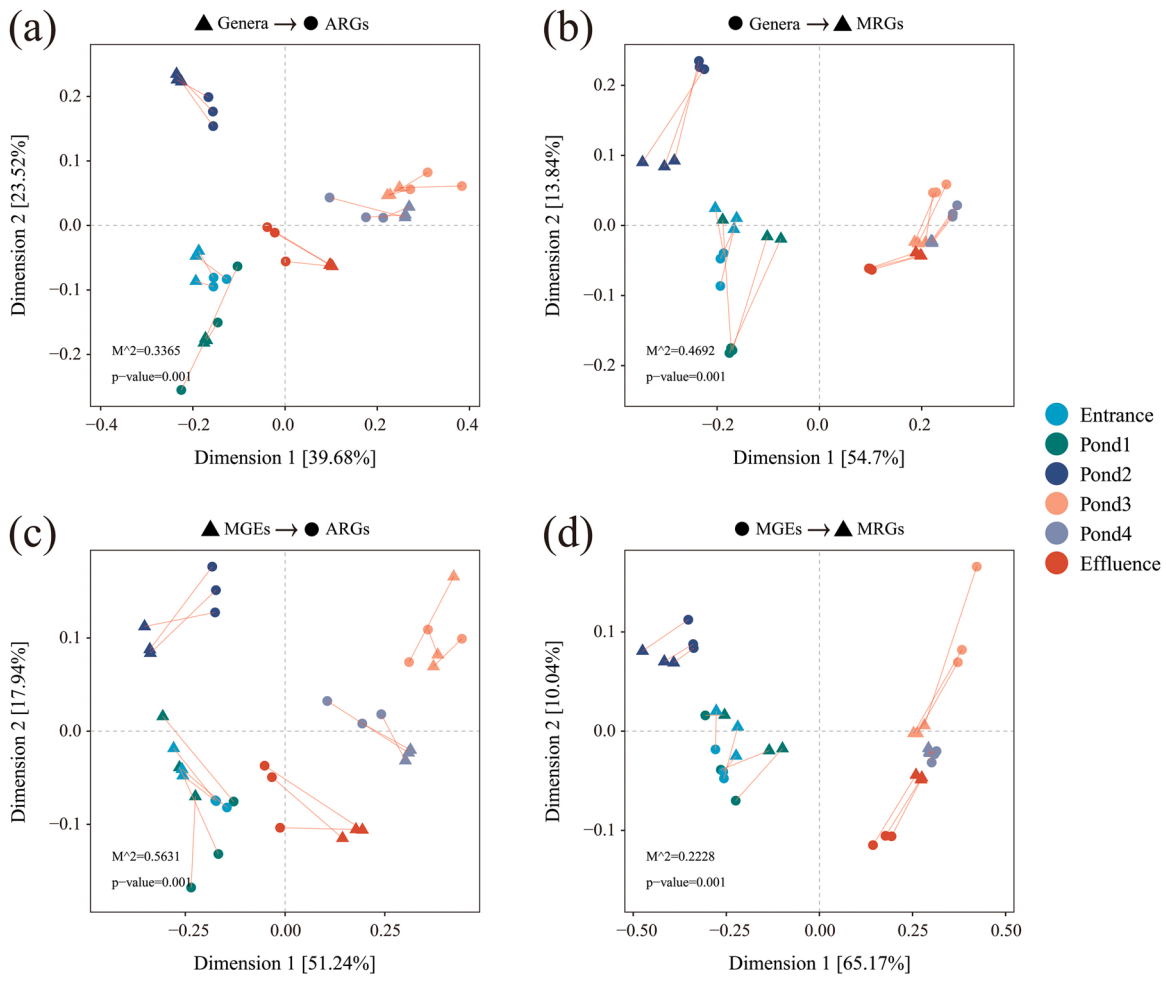

Fig. 4. Procrustes analysis with Spearman correlations displaying significant correlations between (a) genera and antibiotic resistance genes (ARGs), (b) genera and heavy metal(loid) resistance genes (MRGs), (c) mobile gene elements (MGEs) and ARGs, and (d) MGEs and MRGs. In the passive treatment of coal source acid mine drainage, the six sample sites were at the entrance of the first pond and the effluences of five ponds, named as Entrance, Pond1, Pond2, Pond3, Pond4, and Effluence, respectively.

by *arsH* (As resistance), *ruvB* (Cr–selenium (Se)–tellurium (Te) resistance), *dpsA* (Fe resistance), and *arsA* (As–Sb resistance). Total MRGs abundance decreased from 135.55 × /Gb at the influent to 50.859 × /Gb in the effluent, a decrease of 62.48%.

Fig. 2d and Table S5 show MGEs characteristics and variations. Six types of MGEs were detected, including those for integrase, insertion sequences, qacEdelta, plasmid, transposition module, and transposase. In addition, 29 subtypes of MGEs were detected, of which *IS91* and *tnpA* had the highest relative abundances, accounting for over 75% in all sampling sites. Similar to ARGs and MRGs, total MGEs abundance decreased from 501.005 × /Gb at the influent to 198.438 × /Gb in the effluent, a decrease of 60.39%.

3.3. Correlations between antibiotic resistance genes, heavy metal(loid) resistance genes, mobile gene elements and microbial communities

Fig. 3a and Table S6 show the MGEs–ARGs–MRGs (MAM) network, and Fig. 3b and Table S7 show the Genera–ARGs–MRGs (GAM) network. Structural properties (including clustering coefficient, average path length, and network diameter) of the real-world network were greater than those of an identically sized random Erdös–Réyni network (Tables S8 and S9), which suggested that the real network was non-randomly distributed and had a highly connected topological structure.

In the MAM network, 97 nodes (including 29 for ARGs, 32 for MRGs, and 17 for MGEs) formed 215 edges (including 81 ARG–MGE and 134 MRG–MGE edges). Among the 29 ARGs, there were 19 multidrug-related ARGs and four beta-lactam-related ARGs. Among the 32 MRGs, there were four As-related MRGs (1 As–Sb-related MRG), five Cu-related MRGs, four Fe-related MRGs, and five Hg-related MRGs. Among the 215 edges, 81 were the ARG–MGE type, within which multidrug-related ARGs accounted for the most edges at 51. By comparison, 134 edges were the MRG–MGE type, including 22 Cu-related MRGs, 17 Fe-related MRGs, 21 Hg-related MRGs, and 19 As-related MRGs. In addition, multi-resistance genes (mainly *arsA* and *ruvB*) accounted for 43 edges. The four MGEs that correlated with the most RGs were *IS26* (19 ARGs and 9 MRGs), *istA5* (11 ARGs and 17 MRGs), *tnpA2* (9 ARGs and 13 MRGs), and *ISRj1* (10 ARGs and 12 MRGs). Most MGEs were significantly positively correlated with more MRGs than ARGs. The exception was *IS26*, which was correlated with 19 ARGs but only nine MRGs.

In the GAM network, the multidrug-related ARG multidrug_ABC_transporter had the most edges with 28 genera, including several typical AMD species such as *Ferrovum*, *Leptospirillum*, *Acidicaldus*, *Acidobacterium*, *Acidibacillus*, *Metallibacterium*, and *Desulfurispora*. The As-related MRG *pstB* was also significantly positively correlated with 28 genera. The genus with the most connections with RGs was *Acinetobacter*, which connected with 30 RGs resistant to nine types of heavy metal(loid)s and 21 types of antibiotics. The genera *Desulfitobacterium* (20 ARGs and 8 MRGs), *Granulicella* (12 ARGs and 9 MRGs), *Syntrophobacter* (12 ARGs and 7 MRGs), and *Acidiphilium* (4 ARGs and 11 MRGs) also had high numbers of connections. Those genera could be

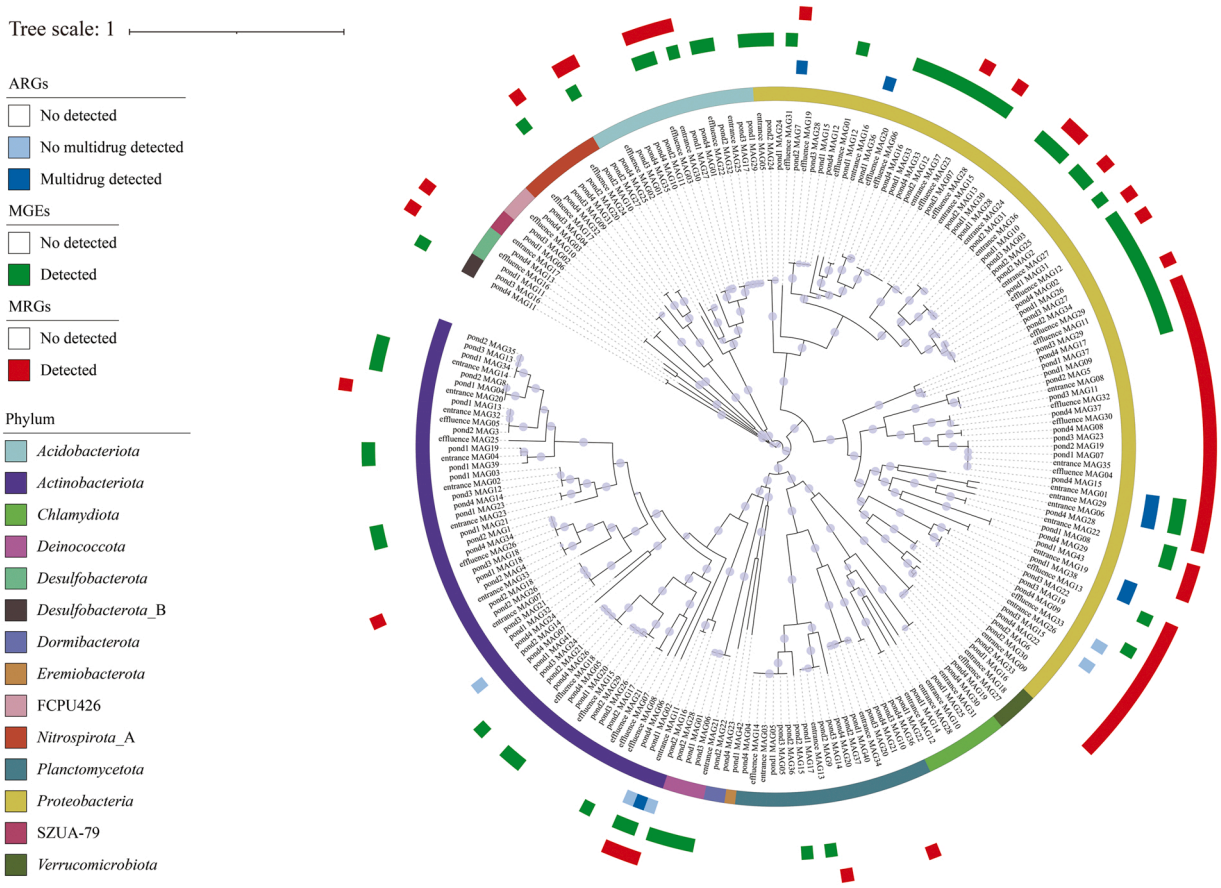

Fig. 5. Phylogenetic tree of bacterial metagenome-assembled genomes (MAGs) and loading of resistance genes, with MAG completeness > 70% and contamination < 5%. From inner to outer circles, colored bars of first circle represent the phyla of every MAG, blue bars of the second circle represent MAGs carrying antibiotic resistance genes (ARGs), green bars of the third circle represent MAGs carrying mobile gene elements (MGEs), and red bars of the fourth circle represent MAGs carrying heavy metal(loid) resistance genes (MRGs).

potential carriers of many types of resistance to antibiotics (such as multidrug, beta-lactam, aminoglycoside) and heavy metal(loid)s (such as As, Cu, Fe, and Zn).

The Procrustes analysis based on relative abundances of genera, ARGs, MRGs, and MGEs showed that microbial communities were nearly equally correlated with ARGs ($M^2 = 0.3365$, $p = 0.001$, Fig. 4a) and MRGs ($M^2 = 0.4692$, $p = 0.001$, Fig. 4b). Although MGEs correlated closely with both ARGs ($M^2 = 0.5631$, $p = 0.001$, Fig. 4c) and MRGs ($M^2 = 0.2228$, $p = 0.001$, Fig. 4d), the smaller value of M^2 between MGEs and MRGs indicated the driving effect of MGEs on MRGs was stronger than on ARGs.

Spearman correlation analysis (Fig. S3) indicated that most ARGs were weakly or significantly negatively correlated with heavy metal (loid)s. By contrast, several MRGs were significantly positively correlated with not only corresponding metal(loid)s but also other metal (loid)s, including *pstB* (As resistance), *merP* (Hg resistance), *merR* (Hg resistance), and several multiresistance genes such as *cueA*, *modC*, *wtpC*, and *nia*. RDA analysis (Fig. S4) also revealed similar results, most ARGs and MRGs exhibited opposite relationship with heavy metal(loid)s.

3.4. Resistance gene load at the genome level

Metagenome assembly and binning were conducted to determine the RG load at the genome level. A total of 215 high-quality MAGs (contamination < 5%, completeness > 70%) were recovered from 18 samples at the six sampling sites, including MAGs for 209 bacteria and six archaea (Fig. 5 and Table S10). Of the six archaea MAGs, only one contained a Cu-related MRG. Of the bacterial MAGs, 101 contained at least one type of RG or MGE. Multidrug-related ARGs also dominated the antibiotic resistome at the genome level, with eight of the 13 ARG-containing MAGs containing at least one multidrug-related ARGs (Table S11).

The six MAGs with the most RGs were annotated as potential pathogenic bacteria, including one from *Pseudomonas* (entrance_MAG01), three from *Mycobacterium* (entrance_MAG11 and pond1_MAG02, annotated as *M. numidiamassiliense*, and pond2_MAG16) and two from *Acinetobacter* (entrance_MAG06 annotated as *A. junii* and entrance_MAG29 annotated as *A. guillouiae*). Entrance_MAG01 contained one MGE and 25 RGs, with resistance to two antibiotics (multidrug and bacitracin) and 12 heavy metal(loid)s. Entrance_MAG11 and pond1_MAG02 both included six MGEs and 13 RGs, with resistance to four antibiotics (multidrug, quinolone, rifamycin, and aminoglycoside), and four heavy metal(loid)s. Pond2_MAG16 contained 10 RGs, with resistance to two antibiotics (aminoglycoside, quinolone) and four heavy metal(loid)s. Entrance_MAG06 included two MGEs and eight RGs, with resistance to multidrug and two heavy metal(loid)s. Entrance_MAG29 contained one MEG and 14 RGs, with resistance to three antibiotics (multidrug, beta-lactam, and aminoglycodise) and four heavy metal(loid)s.

4. Discussion

4.1. Coal source acid mine drainage environment contained a multidrug-dominated antibiotic resistome and a highly diverse heavy metal(loid)s resistome

The antibiotic resistome of the coal source AMD in this study was

dominated by multidrug resistance (Fig. 2a and Fig. 2b), which is consistent with the results of Yi et al. [72]. Zhao et al. [76] and Malik et al. [39] also found multidrug-dominated resistomes in a slightly acidic, As- and Cu-polluted farmland environment and a low-pH soil environment without obvious metal contamination, respectively. Since multidrug-type resistance genes accounted for more than 65% of all sampling sites in this study, it was suggested that a multidrug-resistance-dominated antibiotic resistome likely cooperated with microbial communities to adapt the AMD environment. High occupation of multidrug-related genes might be attributed to their multiple functions, especially in acid resistance and metal(loid) resistance. Some multidrug-resistant ARGs can form tripartite-like organizations, which allow gram-negative bacteria to resist acid stress and maintain pH homeostasis [65]. For example, *emrB–mdtB–tolC* can help *Escherichia coli* survive under acid stress by regulating the expression of *gadAB*, a key component of acid resistance [20,57]. The genes *mdtB* and *mdtC* can help hosts resist Zn [33], while hosts with *mexI* can resist vanadium (V) [2]. Additionally, multidrug-related organizations have other functions, including biofilm formation, quorum sensing, and detoxification [4,44,74].

In other studies, rifamycin-, glycopeptide aminocoumarin-, and macrolide-related resistance were the main antibiotic characters in a copper mine tailing-polluted soil [31], and MLS- (macrolides-lincosamidsstreptogramins-), vancomycin-, and aminoglycoside-related resistance dominated the antibiotic resistome in a gold tailing-polluted farmland [53]. Therefore, further investigations are needed to clarify which key factors regulate antibiotic resistome characteristics in mine environments.

Compared with the antibiotic resistome, the coal source AMD contained a more diverse heavy metal(loid) resistome dominated by Hg-, multimetal(loid)s-, As-, and Fe-resistance genes. Some of the most abundant MRGs, including *merA* (Hg resistance), *arsA* (As–Sb resistance), *arsH* (As resistance), *ruvB* (Cr–Se–Te resistance), and *dpsA* (Fe resistance), provide resistance to more than one type of metal(loid). *MerA* is mercuric reductase, which can convert toxic Hg^{2+} to the less toxic, relatively inert metallic Hg^0 [56]. In addition, *MerA* has a weak reduction ability toward Au^{3+} and Au^{+} [64]. The gene *arsA* encodes a catalytic subunit of a pump protein, and it can move As and Sb through the membrane-spanning arsB protein, while the gene *arsH* catalyzes the NADPH-dependent reduction of Fe, Cr, and As [71]. The gene *ruvB* is a multimetal resistance gene with resistance to Cr, Se, and Te. The Fe-related *dpsA* encodes a protein that can protect chromosomal DNA against oxidative damage, whose expression increases under nutrient deficiency conditions, such as nitrogen or phosphorus limitation [41]. AMD is a typical oligotrophic environment [16], and thus, the enrichment of *dpsA* can help microorganisms survive under such a low-nutrient condition. Like multidrug-resistance-related ARGs, the multifunctional metal(loid)-resistance-related MRGs also likely helped microbial communities adapt to the coal source AMD environment.

4.2. Mobile gene elements were the primary drivers of multifunctional resistance genes in the coal source acid mine drainage

Compared with MGEs, microbial communities are generally considered to be more important in driving the dynamics of resistomes. However, in the AMD environment we investigated, M^2 value between MGEs and MRGs (0.2228, $p = 0.001$) was smaller than that between microbial community and MRGs (0.4692, $p = 0.001$), suggesting MGEs were more critical in driving the dynamics of MRGs than microbial communities. Microorganisms generally acquire new resistance through horizontal gene transfer (HGT) mediated by MGEs under selection pressure and thus adapt to new ecological niches [7]. In the MAM network (Fig. 3a and Supplementary Table S6), MRGs were more frequently correlated with MGEs such as *tnpA*, *tnpA2*, *IS91*, *ICSau1*, *istA*, and *intI1*, compared with ARGs. Therefore, as indicated by the smaller M^2 value of 0.2228 (Fig. 4d) than that of 0.5631 (Fig. 4c) in the Procrustes analysis, microorganisms tended to exchange more MRGs than ARGs through HGT to improve survival under metal(loid)s pressure. The more significant horizontal transfer of MRGs might be because MRGs are more specialized than ARGs in resisting heavy metal(loid) pressure, which also explains the higher MRGs abundance than ARGs. The higher relative abundances of MGEs than MRGs and ARGs could be because, besides antibiotic and heavy metal(loid) resistance, microorganisms also need to acquire or reinforce other abilities by HGT, such as acid tolerance, materials transport and metabolism to adapt to harsh AMD environments [17,24].

4.3. Coal source acid mine drainage contained several resistant gene-carrying potential pathogens

Most potential multi-RG carriers were typical acidophilic heterotrophic microorganisms, including *Acinetobacter*, *Desulfitobacterium*, *Granulicella*, *Syntrophobacter*, *Acidiphilium*, *Acidocella*, and *Acidibacter* (Fig. 3b), which are frequently detected in acidic environments [16,26]. Carrying multiple MRGs and multifunctional RND-type (resistance-nodulation-cell division) RGs allowed them to better survive in the extremely acidic, multimetal(loid)-enriched AMD environment.

By binning, the six MAGs that carried the most RGs were also annotated as potential pathogenic genera spp., namely *Pseudomonas*, *Mycobacterium*, and *Acinetobacter*. Species of those genera inhabit a wide variety of environments, and many are pathogens or opportunistic pathogens of humans, animals, and plants [21,51,66]. In addition to diverse types of resistance, many species are also acid tolerant. Several hydrothermal vent-sourced *Pseudomonas* strains can adapt to acidity and antibiotics [12], and *P. aeruginosa* is acid tolerant and cause nosocomial infections [34,42]. *Mycobacterium avium* can survive from pH < 3 [8], and *M. tuberculosis* and *M. smegmatis* can survive at pH 4.5 by down-regulation of transmembrane transporter activity and up-regulation of enzymes involved in fatty acid metabolism [43,55,59]. *Acinetobacter* was found in the skin of a Perez's frog that inhabited an acidic, metal-polluted site [52].

Pathogens resistant to different antibiotics are a worldwide public health threat [5]. In addition, heavy metal(loid)s such as As, Cd, Cu, Hg, silver (Ag), Te, and Zn have been used in clinics because they may partly replace antibiotic therapy [14]. Therefore, potential risk of heavy metal (loid) therapy failure caused by heavy metal(loid)-resistant pathogens is also a concern [75]. Moreover, the threats of infections caused by pathogens carrying multi-RGs might be more severe than single-resistance pathogen infection. The problem may worsen if pathogens can survive in extreme environments. For example, a multidrug-resistant and mercury-tolerant pathogenic *E. coli* was recovered from a mining-affected river, and its resistance to heavy metals was thought to be related to environmental pollution by mining activities [23].

Although only entrance_MAG06 was annotated similarly to *A. junii*, a pathogen of the urinary tract [1], the possibility still exists as the other five MAGs may be potential pathogens. Besides, concern remains because HGT events are more likely to occur between phylogenetically related species and cause RGs to transfer to corresponding pathogenic members in the same genus [19]. Thus, if AMD is discharged into the surrounding environment without proper treatment, multi-RG carrying MAGs might increase the risk of ARG diffusion, leading to therapy failure and threatening public health. Consequently, more attention should be paid to potential multi-RG carriers surviving in such acidic multimetal(loid) environments.

4.4. Suggestion for passive treatment of acid mine drainage

Reported studies on AMD passive treatment have not evaluate effects on resistomes yet. In this study, from the influent to the effluent of a passive treatment system, relative abundance of ARGs, MRGs, and MGEs decreased to different degrees. A possible reason is that co-selection

effects on RGs induced by heavy (metal)loids were less critical than the adverse effects of low nutrients [25] because many resistance mechanisms (especially efflux pumps) are energetically costly. In addition, HGT efficiency might also decrease because acid solutions and heavy metal(loid)s can prevent gene transfer and the uptake of naked DNA in AMD [24,69]. AMD passive treatment systems operate differently under various environmental parameters. Thus the microbial communities and resistomes of different sites are expected to be somewhat different from the results in this study. Therefore, more studies are warranted to address the resistomes dynamics under AMD passive treatment to provide guidance and improve AMD treatment.

5. Conclusions

Current studies on resistome characteristics of typical metal(loid) mine environments have overlooked coal mine environments, which may contain many different types of metal(loid)s and thus are potential significant RG reservoirs. This study used metagenomic techniques and geochemical measurements to investigate resistome characteristics and dynamics in a passive coal source AMD treatment system. The major findings include: (1) the multidrug efflux mechanism dominated the antibiotic resistome, and the heavy metal(loid) resistome had a high diversity; (2) the microbial community survives in the acidic, multimetal(loid)-enriched environment likely through horizontal transfer of multifunctional RGs; and (3) the occurrence of multi-RG-carrying potential pathogens indicated that discharge of coal source AMD must be controlled to minimize risks to human health and ARG environmental proliferation. Additional investigations on AMD passive treatment systems with different metal(loid)s and SO_4^{2-} content should be conducted to guide AMD treatment.

Funding

This work was supported by grants from the National Key Research and Development Project of China (2018YFC1802601), the National Nature Science Foundation of China (91851206, 41877400), Startup Funding of the Chinese Academy of Sciences (2017-020), the Joint Funds of Innovation Academy for Green Manufacture, Chinese Academy of Sciences (IAGM2020C24),the CAS Engineering Laboratory for Advanced Microbial Technology of Agriculture, Chinese Academy of Sciences (KFJ-PTXM-016), CAS–NSTDA Joint Research Project (153211KYSB20200039), the State Key Laboratory of Environmental Geochemistry (SKLEG2018911), and the State Key Laboratory of Microbial Technology Foundation (M2017-01).

CRediT authorship contribution statement

Qiang Huang: Writing – original draft, Methodology; **Ye Huang:** Visualization, Software; **Bao Li, Xiutong Li, and Yuan Guo:** Validation, Investigation; **Zhen Jiang, Xiaoling Liu, and Zhenni Yang:** Data curation, Resources; **Tangfu Xiao, Zengping Ning, Chengying Jiang, and Likai Hao:** Supervision, Funding acquisition, Conceptualization.

Declaration of Competing Interest

The authors declare that they have no known competing financial interests or personal relationships that could have appeared to influence the work reported in this paper.

Data Availability

The data that has been used is confidential.

Acknowledgements

We thank Fan Yuhong, Yang Xiuqun, and Yang Fei for their technical assistance with OES, ICP-MS, and IC measurements. We also thank Wan Liu for data submission.

Appendix A. Supporting information

Supplementary data associated with this article can be found in the online version at doi:10.1016/j.jhazmat.2023.130898.

References

[1] Abo-Zed, A., Yassin, M., Phan, T., 2020. Acinetobacter junii as a rare pathogen of urinary tract infection. Urol Case Rep 32, 101209. https://doi.org/10.1016/j.eucr.2020.101209.
[2] Aendekerk, S., Ghysels, B., Cornelis, P., Baysse, C., 2002. Characterization of a new efflux pump, MexGHI-OpmD, from Pseudomonas aeruginosa that confers resistance to vanadium. Microbiology 148 (Pt 8), 2371–2381. https://doi.org/10.1099/00221287-148-8-2371.
[3] Akcil, A., Koldas, S., 2006. Acid Mine Drainage (AMD): causes, treatment and case studies. J Clean Prod 14 (12), 1139–1145. https://doi.org/10.1016/j.jclepro.2004.09.006.
[4] Alav, I., Kobylka, J., Kuth, M.S., Pos, K.M., Picard, M., Blair, J.M.A., et al., 2021. Structure, assembly, and function of tripartite efflux and type 1 secretion systems in gram-negative bacteria. Chem Rev 121 (9), 5479–5596. https://doi.org/10.1021/acs.chemrev.1c00055.
[5] Ayobami, O., Brinkwirth, S., Eckmanns, T., Markwart, R., 2022. Antibiotic resistance in hospital-acquired ESKAPE-E infections in low- and lower-middle-income countries: a systematic review and meta-analysis. Emerg Microbes Infect 11 (1), 443–451. https://doi.org/10.1080/22221751.2022.2030196.
[6] Berendonk, T.U., Manaia, C.M., Merlin, C., Fatta-Kassinos, D., Cytryn, E., Walsh, F., et al., 2015. Tackling antibiotic resistance: the environmental framework. Nat Rev Microbiol 13 (5), 310–317. https://doi.org/10.1038/nrmicro3439.
[7] Blair, J.M.A., Webber, M.A., Baylay, A.J., Ogbolu, D.O., Piddock, L.J.V., 2015. Molecular mechanisms of antibiotic resistance. Nat Rev Microbiol 13 (1), 42–51. https://doi.org/10.1038/nrmicro3380.
[8] Bodmer, T., Miltner, E., Bermudez, L.E., 2000. Mycobacterium avium resists exposure to the acidic conditions of the stomach. FEMS Microbiol Lett 182 (1), 45–49. https://doi.org/10.1111/j.1574-6968.2000.tb08871.x.
[9] Bokulich, N.A., Kaehler, B.D., Rideout, J.R., Dillon, M., Bolyen, E., Knight, R., et al., 2018. Optimizing taxonomic classification of marker-gene amplicon sequences with QIIME 2's q2-feature-classifier plugin. Microbiome 6 (1), 90. https://doi.org/10.1186/s40168-018-0470-z.
[10] Bolger, A.M., Lohse, M., Usadel, B., 2014. Trimmomatic: a flexible trimmer for Illumina sequence data. Bioinformatics 30 (15), 2114–2120. https://doi.org/10.1093/bioinformatics/btu170.
[11] Bolyen, E., Rideout, J.R., Dillon, M.R., Bokulich, N.A., Abnet, C.C., Al-Ghalith, G.A., et al., 2019. Reproducible, interactive, scalable and extensible microbiome data science using QIIME 2. Nat Biotechnol 37 (8), 852–857. https://doi.org/10.1038/s41587-019-0209-9.
[12] Bravakos, P., Mandalakis, M., Nomikou, P., Anastasiou, T.I., Kristoffersen, J.B., Stavroulaki, M., et al., 2021. Genomic adaptation of Pseudomonas strains to acidity and antibiotics in hydrothermal vents at Kolumbo submarine volcano, Greece. Sci Rep 11 (1). https://doi.org/10.1038/s41598-020-79359-y.
[13] Callahan, B.J., McMurdie, P.J., Rosen, M.J., Han, A.W., Johnson, A.J., Holmes, S.P., 2016. DADA2: High-resolution sample inference from Illumina amplicon data. Nat Methods 13 (7), 581–583. https://doi.org/10.1038/nmeth.3869.
[14] Cheeseman, S., Christofferson, A.J., Kariuki, R., Cozzolino, D., Daeneke, T., Crawford, R.J., et al., 2020. Antimicrobial metal nanomaterials: from passive to stimuli-activated applications. Adv Sci 7 (10), 1902913. https://doi.org/10.1002/advs.201902913.
[15] Chen, H., Xiao, T., Ning, Z., Li, Q., Xiao, E., Liu, Y., et al., 2020. In-situ remediation of acid mine drainage from abandoned coal mine by filed pilot-scale passive treatment system: Performance and response of microbial communities to low pH and elevated Fe. Bioresour Technol 317, 123985. https://doi.org/10.1016/j.biortech.2020.123985.
[16] Chen, L.X., Huang, L.N., Méndez-García, C., Kuang, J.L., Hua, Z.S., Liu, J., et al., 2016. Microbial communities, processes and functions in acid mine drainage ecosystems. Curr Opin Biotechnol 38, 150–158. https://doi.org/10.1016/j.copbio.2016.01.013.
[17] Chen, Z., Liu, W.S., Zhong, X., Zheng, M., Fei, Y.H., He, H., et al., 2021. Genome- and community-level interaction insights into the ecological role of archaea in rare earth element mine drainage in South China. Water Res 201, 117331. https://doi.org/10.1016/j.watres.2021.117331.
[18] Crofts, T.S., Gasparrini, A.J., Dantas, G., 2017. Next-generation approaches to understand and combat the antibiotic resistome. Nat Rev Microbiol 15 (7), 422–434. https://doi.org/10.1038/nrmicro.2017.28.
[19] Daubin, V., Szöllősi, G.J., 2016. Horizontal gene transfer and the history of life. Cold Spring Harb Perspect Biol 8 (4), a018036. https://doi.org/10.1101/cshperspect.a018036.
[20] Deininger, K.N., Horikawa, A., Kitko, R.D., Tatsumi, R., Rosner, J.L., Wachi, M., et al., 2011. A requirement of TolC and MDR efflux pumps for acid adaptation and GadAB induction in Escherichia coli. Plos One 6 (4), e18960. https://doi.org/10.1371/journal.pone.0018960.

[21] Forbes, B.A., 2017. Mycobacterial taxonomy. J Clin Microbiol 55 (2), 380–383. https://doi.org/10.1128/jcm.01287-16.
[22] Fu, L., Niu, B., Zhu, Z., Wu, S., Li, W., 2012. CD-HIT: accelerated for clustering the next-generation sequencing data. Bioinformatics 28 (23), 3150–3152. https://doi.org/10.1093/bioinformatics/bts565.
[23] Gaeta, N.C., de Carvalho, D.U., Fontana, H., Sano, E., Moura, Q., Fuga, B., et al., 2022. Genomic features of a multidrug-resistant and mercury-tolerant environmental Escherichia coli recovered after a mining dam disaster in South America. Sci Total Environ 823, 153590. https://doi.org/10.1016/j.scitotenv.2022.153590.
[24] Guo, J., Wang, Q., Wang, X., Wang, F., Yao, J., Zhu, H., 2015. Horizontal gene transfer in an acid mine drainage microbial community. BMC Genom 16 (1), 496. https://doi.org/10.1186/s12864-015-1720-0.
[25] Herren, C.M., Baym, M., 2022. Decreased thermal niche breadth as a trade-off of antibiotic resistance. ISME J. https://doi.org/10.1038/s41396-022-01235-6.
[26] Huang, L.N., Kuang, J.L., Shu, W.S., 2016. Microbial ecology and evolution in the acid mine drainage model system. Trends Microbiol 24 (7), 581–593. https://doi.org/10.1016/j.tim.2016.03.004.
[27] Hyatt, D., Chen, G.L., Locascio, P.F., Land, M.L., Larimer, F.W., Hauser, L.J., 2010. Prodigal: prokaryotic gene recognition and translation initiation site identification. BMC Bioinforma 11, 119. https://doi.org/10.1186/1471-2105-11-119.
[28] Imran, M., Das, K.R., Naik, M.M., 2019. Co-selection of multi-antibiotic resistance in bacterial pathogens in metal and microplastic contaminated environments: An emerging health threat. Chemosphere 215, 846–857. https://doi.org/10.1016/j.chemosphere.2018.10.114.
[29] Ji, X., Shen, Q., Liu, F., Ma, J., Xu, G., Wang, Y., et al., 2012. Antibiotic resistance gene abundances associated with antibiotics and heavy metals in animal manures and agricultural soils adjacent to feedlots in Shanghai; China. J Hazard Mater 235–236, 178–185. https://doi.org/10.1016/j.jhazmat.2012.07.040.
[30] Jia, B., Raphenya, A.R., Alcock, B., Waglechner, N., Guo, P., Tsang, K.K., et al., 2017. CARD 2017: expansion and model-centric curation of the comprehensive antibiotic resistance database. Nucleic Acids Res 45 (D1), D566–d573. https://doi.org/10.1093/nar/gkw1004.
[31] Jiang, X., Liu, W., Xu, H., Cui, X., Li, J., Chen, J., et al., 2021. Characterizations of heavy metal contamination, microbial community, and resistance genes in a tailing of the largest copper mine in China. Environ Pollut 280, 116947. https://doi.org/10.1016/j.envpol.2021.116947.
[32] Johnson, D.B., Hallberg, K.B., 2003. The microbiology of acidic mine waters. Res Microbiol 154 (7), 466–473. https://doi.org/10.1016/S0923-2508(03)00114-1.
[33] Lee, L.J., Barrett, J.A., Poole, R.K., 2005. Genome-wide transcriptional response of chemostat-cultured Escherichia coli to zinc. J Bacteriol 187 (3), 1124–1134. https://doi.org/10.1128/jb.187.3.1124-1134.2005.
[34] Lewenza, S., Johnson, L., Charron-Mazenod, L., Hong, M., O'Grady, H.M., 2020. Extracellular DNA controls expression of Pseudomonas aeruginosa genes involved in nutrient utilization, metal homeostasis, acid pH tolerance and virulence. J Med Microbiol 69 (6), 895–905. https://doi.org/10.1099/jmm.0.001184.
[35] Li, D., Liu, C.M., Luo, R., Sadakane, K., Lam, T.W., 2015. MEGAHIT: an ultra-fast single-node solution for large and complex metagenomics assembly via succinct de Bruijn graph. Bioinformatics 31 (10), 1674–1676. https://doi.org/10.1093/bioinformatics/btv033.
[36] Li, L.G., Xia, Y., Zhang, T., 2017. Co-occurrence of antibiotic and metal resistance genes revealed in complete genome collection. ISME J 11 (3), 651–662. https://doi.org/10.1038/ismej.2016.155.
[37] Li, X., Rensing, C., Vestergaard, G., Arumugam, M., Nesme, J., Gupta, S., et al., 2021. Metagenomic evidence for co-occurrence of antibiotic, biocide and metal resistance genes in pigs. Environ Int 158, 106899. https://doi.org/10.1016/j.envint.2021.106899.
[38] Liu, T., Liu, S., 2020. The impacts of coal dust on miners' health: A review. Environ Res 190, 109849. https://doi.org/10.1016/j.envres.2020.109849.
[39] Malik, A.A., Thomson, B.C., Whiteley, A.S., Bailey, M., Griffiths, R.I., 2017. Bacterial physiological adaptations to contrasting edaphic conditions identified using landscape scale metagenomics. mBio 8 (4). https://doi.org/10.1128/mBio.00799-17.
[40] Mazhar, S.H., Li, X., Rashid, A., Su, J., Xu, J., Brejnrod, A.D., et al., 2021. Co-selection of antibiotic resistance genes, and mobile genetic elements in the presence of heavy metals in poultry farm environments. Sci Total Environ 755 (Pt 2), 142702. https://doi.org/10.1016/j.scitotenv.2020.142702.
[41] Michel, K.P., Berry, S., Hifney, A., Kruip, J., Pistorius, E.K., 2003. Adaptation to iron deficiency: a comparison between the cyanobacterium Synechococcus elongatus PCC 7942 wild-type and a DpsA-free mutant. Photosynth Res 75 (1), 71–84. https://doi.org/10.1023/a:1022459919040.
[42] Naveed, M., Chaudhry, Z., Bukhari, S.A., Meer, B., Ashraf, H., 2020. Antibiotics resistance mechanism. In: Hashmi, M.Z. (Ed.), Antibiotics and Antimicrobial Resistance Genes in the Environment. Elsevier, pp. 292–312. https://doi.org/10.1016/B978-0-12-818882-8.00019-X.
[43] O'Brien, L.M., Gordon, S.V., Roberts, I.S., Andrew, P.W., 1996. Response of Mycobacterium smegmatis to acid stress. FEMS Microbiol Lett 139 (1), 11–17. https://doi.org/10.1111/j.1574-6968.1996.tb08173.x.
[44] Okusu, H., Ma, D., Nikaido, H., 1996. AcrAB efflux pump plays a major role in the antibiotic resistance phenotype of Escherichia coli multiple-antibiotic-resistance (Mar) mutants. J Bacteriol 178 (1), 306–308. https://doi.org/10.1128/jb.178.1.306-308.1996.
[45] Pal, C., Asiani, K., Arya, S., Rensing, C., Stekel, D.J., Larsson, D.G.J., et al., 2017. Metal resistance and its association with antibiotic resistance. Adv Microb Physiol 70, 261–313. https://doi.org/10.1016/bs.ampbs.2017.02.001.
[46] Pal, C., Bengtsson-Palme, J., Rensing, C., Kristiansson, E., Larsson, D.G., 2014. BacMet: antibacterial biocide and metal resistance genes database. Nucleic Acids Res 42 (Database issue), D737–D743. https://doi.org/10.1093/nar/gkt1252.
[47] Parks, D.H., Chuvochina, M., Rinke, C., Mussig, A.J., Chaumeil, P.A., Hugenholtz, P., 2022. GTDB: an ongoing census of bacterial and archaeal diversity through a phylogenetically consistent, rank normalized and complete genome-based taxonomy. D785-d794 Nucleic Acids Res 50 (D1). https://doi.org/10.1093/nar/gkab776.
[48] Parks, D.H., Imelfort, M., Skennerton, C.T., Hugenholtz, P., Tyson, G.W., 2015. CheckM: assessing the quality of microbial genomes recovered from isolates, single cells, and metagenomes. Genome Res 25 (7), 1043–1055. https://doi.org/10.1101/gr.186072.114.
[49] Pärnänen, K., Karkman, A., Hultman, J., Lyra, C., Bengtsson-Palme, J., Larsson, D. G.J., et al., 2018. Maternal gut and breast milk microbiota affect infant gut antibiotic resistome and mobile genetic elements. Nat Commun 9 (1), 3891. https://doi.org/10.1038/s41467-018-06393-w.
[50] Patro, R., Duggal, G., Love, M.I., Irizarry, R.A., Kingsford, C., 2017. Salmon provides fast and bias-aware quantification of transcript expression. Nat Methods 14 (4), 417–419. https://doi.org/10.1038/nmeth.4197.
[51] Peix, A., Ramírez-Bahena, M.H., Velázquez, E., 2009. Historical evolution and current status of the taxonomy of genus Pseudomonas. Infect Genet Evol 9 (6), 1132–1147. https://doi.org/10.1016/j.meegid.2009.08.001.
[52] Proença, D.N., Fasola, E., Lopes, I., Morais, P.V., 2021. Characterization of the skin cultivable microbiota composition of the frog pelophylax perezi inhabiting different environments. Int J Environ Res Public Health 18 (5). https://doi.org/10.3390/ijerph18052585.
[53] Qiao, L., Liu, X., Zhang, S., Zhang, L., Li, X., Hu, X., et al., 2021. Distribution of the microbial community and antibiotic resistance genes in farmland surrounding gold tailings: A metagenomics approach. Sci Total Environ 779, 146502. https://doi.org/10.1016/j.scitotenv.2021.146502.
[54] Robeson 2nd, M.S., O'Rourke, D.R., Kaehler, B.D., Ziemski, M., Dillon, M.R., Foster, J.T., et al., 2021. RESCRIPt: Reproducible sequence taxonomy reference database management. PLoS Comput Biol 17 (11), e1009581. https://doi.org/10.1371/journal.pcbi.1009581.
[55] Roxas, B.A., Li, Q., 2009. Acid stress response of a mycobacterial proteome: insight from a gene ontology analysis. Int J Clin Exp Med 2 (4), 309–328.
[56] Rugh, C.L., Wilde, H.D., Stack, N.M., Thompson, D.M., Summers, A.O., Meagher, R. B., 1996. Mercuric ion reduction and resistance in transgenic Arabidopsis thaliana plants expressing a modified bacterial merA gene. Proc Natl Acad Sci USA 93 (8), 3182–3187. https://doi.org/10.1073/pnas.93.8.3182.
[57] Schaffner, S.H., Lee, A.V., Pham, M.T.N., Kassaye, B.B., Li, H., Tallada, S., et al., 2021. Extreme acid modulates fitness trade-offs of multidrug efflux pumps MdtEF-TolC and AcrAB-TolC in Escherichia coli K-12. Appl Environ Microbiol 87 (16), e0072421. https://doi.org/10.1128/aem.00724-21.
[58] Seiler, C., Berendonk, T.U., 2012. Heavy metal driven co-selection of antibiotic resistance in soil and water bodies impacted by agriculture and aquaculture. Front Microbiol 3, 399. https://doi.org/10.3389/fmicb.2012.00399.
[59] Shahbaaz, M., Potemkin, V., Grishina, M., Bisetty, K., Hassan, I., 2020. The structural basis of acid resistance in Mycobacterium tuberculosis: insights from multiple pH regime molecular dynamics simulations. J Biomol Struct Dyn 38 (15), 4483–4492. https://doi.org/10.1080/07391102.2019.1682676.
[60] Song, J., Rensing, C., Holm, P.E., Virta, M., Brandt, K.K., 2017. Comparison of metals and tetracycline as selective agents for development of tetracycline resistant bacterial communities in agricultural soil. Environ Sci Technol 51 (5), 3040–3047. https://doi.org/10.1021/acs.est.6b05342.
[61] Song, J., Rensing, C., Holm, P.E., Virta, M., Brandt, K.K., 2017. Comparison of metals and tetracycline as selective agents for development of tetracycline resistant bacterial communities in agricultural soil. Environ Sci Technol 51 (5), 3040–3047. https://doi.org/10.1021/acs.est.6b05342.
[62] Stepanauskas, R., Glenn, T.C., Jagoe, C.H., Tuckfield, R.C., Lindell, A.H., McArthur, J.V., 2005. Elevated microbial tolerance to metals and antibiotics in metal-contaminated industrial environments. Environ Sci Technol 39 (10), 3671–3678. https://doi.org/10.1021/es048468f.
[63] Stookey, L.L., 1970. Ferrozine—A new spectrophotometric reagent for Iron. Anal Chem 42, 7.
[64] Summers, A.O., Sugarman, L.I., 1974. Cell-free mercury(II)-reducing activity in a plasmid-bearing strain of Escherichia coli. J Bacteriol 119 (1), 242–249. https://doi.org/10.1128/jb.119.1.242-249.1974.
[65] Teelucksingh, T., Thompson, L.K., Cox, G., 2020. The evolutionary conservation of escherichia coli drug efflux pumps supports physiological functions. J Bacteriol 202 (22). https://doi.org/10.1128/jb.00367-20.
[66] Towner, K.J., 2009. Acinetobacter: an old friend, but a new enemy. J Hosp Infect 73 (4), 355–363. https://doi.org/10.1016/j.jhin.2009.03.032.
[67] Uritskiy, G.V., DiRuggiero, J., Taylor, J., 2018. MetaWRAP-a flexible pipeline for genome-resolved metagenomic data analysis. Microbiome 6 (1), 158. https://doi.org/10.1186/s40168-018-0541-1.
[68] Wales, A.D., Davies, R.H., 2015. Co-selection of resistance to antibiotics, biocides and heavy metals, and its relevance to foodborne pathogens. Antibiot (Basel) 4 (4), 567–604. https://doi.org/10.3390/antibiotics4040567.
[69] Wenhua, L., Ruming, Z., Zhixiong, X., Xiangdong, C., Ping, S., 2003. Effects of La3 + on growth, transformation, and gene expression of Escherichia coli. Biol Trace Elem Res 94 (2), 167–177. https://doi.org/10.1385/BTER:94:2:167.
[70] Wozniak, R.A.F., Waldor, M.K., 2010. Integrative and conjugative elements: mosaic mobile genetic elements enabling dynamic lateral gene flow. Nat Rev Microbiol 8 (8), 552–563. https://doi.org/10.1038/nrmicro2382.

[71] Yang, H.C., Rosen, B.P., 2016. New mechanisms of bacterial arsenic resistance. Biomed J 39 (1), 5–13. https://doi.org/10.1016/j.bj.2015.08.003.
[72] Yi, X., Liang, J.L., Su, J.Q., Jia, P., Lu, J.L., Zheng, J., et al., 2022. Globally distributed mining-impacted environments are underexplored hotspots of multidrug resistance genes. ISME J. https://doi.org/10.1038/s41396-022-01258-z.
[73] Yin, X., Jiang, X.T., Chai, B., Li, L., Yang, Y., Cole, J.R., et al., 2018. ARGs-OAP v2.0 with an expanded SARG database and Hidden Markov Models for enhancement characterization and quantification of antibiotic resistance genes in environmental metagenomes. Bioinformatics 34 (13), 2263–2270. https://doi.org/10.1093/bioinformatics/bty053.
[74] Yu, E.W., McDermott, G., Zgurskaya, H.I., Nikaido, H., Koshland Jr., D.E., 2003. Structural basis of multiple drug-binding capacity of the AcrB multidrug efflux pump. Science 300 (5621), 976–980. https://doi.org/10.1126/science.1083137.
[75] Zagui, G.S., Moreira, N.C., Santos, D.V., Darini, A.L.C., Domingo, J.L., Segura-Muñoz, S.I., et al., 2021. High occurrence of heavy metal tolerance genes in bacteria isolated from wastewater: A new concern? Environ Res 196, 110352. https://doi.org/10.1016/j.envres.2020.110352.
[76] Zhao, X., Shen, J.P., Zhang, L.M., Du, S., Hu, H.W., He, J.Z., 2020. Arsenic and cadmium as predominant factors shaping the distribution patterns of antibiotic resistance genes in polluted paddy soils. J Hazard Mater 389, 121838. https://doi.org/10.1016/j.jhazmat.2019.121838.
[77] Zhao, Y., Cocerva, T., Cox, S., Tardif, S., Su, J.Q., Zhu, Y.G., et al., 2019. Evidence for co-selection of antibiotic resistance genes and mobile genetic elements in metal polluted urban soils. Sci Total Environ 656, 512–520. https://doi.org/10.1016/j.scitotenv.2018.11.372.
[78] Zhou, L., Xu, P., Gong, J., Huang, S., Chen, W., Fu, B., et al., 2022. Metagenomic profiles of the resistome in subtropical estuaries: Co-occurrence patterns, indicative genes, and driving factors. Sci Total Environ 810, 152263. https://doi.org/10.1016/j.scitotenv.2021.152263.